



Indirect method of measuring glass temperature in a Cold Crucible Induction Melter

G. Barba Rossa, E. Sauvage, P. Brun

► To cite this version:

G. Barba Rossa, E. Sauvage, P. Brun. Indirect method of measuring glass temperature in a Cold Crucible Induction Melter. Electrotechnologies for Material Processing (XVIII International UIE-Congress), Jun 2017, Hannovre, Germany. cea-02338886

HAL Id: cea-02338886

<https://cea.hal.science/cea-02338886>

Submitted on 21 Feb 2020

HAL is a multi-disciplinary open access archive for the deposit and dissemination of scientific research documents, whether they are published or not. The documents may come from teaching and research institutions in France or abroad, or from public or private research centers.

L'archive ouverte pluridisciplinaire **HAL**, est destinée au dépôt et à la diffusion de documents scientifiques de niveau recherche, publiés ou non, émanant des établissements d'enseignement et de recherche français ou étrangers, des laboratoires publics ou privés.

Indirect method of measuring glass temperature in a Cold Crucible Induction Melter

G. Barba Rossa, E. Sauvage, P. Brun

Abstract

This study is concerned with the control and optimization of the vitrification process of High-Level-Waste in a Cold Crucible Induction Melter (CCIM). We developed a new method for the control of glass temperature in the crucible, based on the precise measurement of heat flux through a water-cooled stick immersed into the glass melt. The measuring stick is separated from the flowing hot glass by a cold glass “skull”, ensuring much lower exposure to corrosive conditions than classical thermocouple sensors. This heat flux measurement enables a precise estimate of the glass temperature using a newly designed correlation formula between heat flux and glass temperature. Dimensioning of the measurement stick – size and cooling water supply – was achieved by running coupled 3D numerical simulations of fluid flow, heat transfers and electromagnetics in the CCIM.

Introduction

Material processing involving Cold Crucible Induction Melters needs a precise temperature control using sensors that can withstand strongly corrosive conditions and relatively strong harmonic magnetic fields. Up to now, most of temperature measurements are carried out by means of thermocouple sensors embedded in glove fingers made of noble materials that can tolerate corrosive hot glass flow. In this design, the fingers have to be sufficiently thin and long to get rid of perturbations induced by heat conduction towards the water-cooled stick propping them up. This study focused on the design and testing of an indirect temperature measurement technic based on heat flux measurement, where we derived a temperature estimator using multiphysic modelling of the CCIM, taking into account direct electromagnetic induction inside the melt, glass flow and heat transfers.

1. CCIM modelling and estimator design

1.1. Cold Crucible Induction Melting

Cold Crucible Induction Melters are cooled crucibles into which processed materials are heat-treated by direct electromagnetic induction. In the vitrification process of High-Level-Waste, the glass mixture is strongly agitated by means of an immersed rotating agitator shaft to reach atomic scale entrapment of nuclear wastes and both thermal and chemical homogenization. The use of cold crucibles induction melters is convenient for processing strongly corrosive materials that need high elaboration temperatures. Almost every part of the metallic crucible is water-cooled and thus coated with a relatively cold protecting layer usually called “glass skull”. Instead of being submitted to high temperatures, these cooled elements undergo strong heat transfers from the glass melt to the cooling water.

1.2. Multiphysics modelling

The glass mixture is considered as a local non-polarizable and non-magnetic linear isotropic conductor. The Maxwell equations are written in the quasi-magnetostatic approximation, using the $\mathbf{A} - V$ potentials formulation and are solved in the frequency domain. Enforcing Coulomb gauge, the induction problem is reduced to the following Maxwell-Ampère and charge conservation equations:

$$\nabla^2 \mathbf{A} = \mu_0 \sigma (\nabla V + i2\pi f \mathbf{A}) \quad (1.1)$$

$$\nabla \cdot (\sigma (\nabla V + i2\pi f \mathbf{A})) = 0 \quad (1.2)$$

Parameters appearing in all the equations are gathered in Tab. 1. For the sake of simplicity, we only give typical values since most of the parameters related to glass are temperature-dependent. The external oscillating magnetic field produced by the surrounding inductor is modelled by a uniform vertically oriented field using suitable Dirichlet boundary conditions for the vector potential on the cylindrical lateral boundary of the melt:

$$\mathbf{A} = A_\theta \mathbf{e}_\theta \quad (1.3)$$

where \mathbf{e}_θ is the orthoradial unit vector, and homogeneous Neumann boundary conditions on other boundaries [1, 2]. An inhomogeneous Neumann boundary condition for the scalar potential on every boundary ensures zero face-normal currents (the glass skull is considered as a perfect electrical insulator):

$$\frac{\partial V}{\partial n} = -i2\pi f \mathbf{A} \cdot \mathbf{n} \quad (1.4)$$

where \mathbf{n} is the outward pointing normal unit vector [3]. Thermo-hydraulic modelling assumes an incompressible and laminar flow of glass, considered itself as a Newtonian fluid with temperature-dependent viscosity following Volgel-Fulcher-Tammann (VFT) law:

$$\eta(T) = \eta_0 \exp\left(\frac{B}{R(T-T_v)}\right) \quad (1.5)$$

The Navier-Stokes equations are written under Boussinesq approximation to account for natural convection and Rosseland diffusion approximation for internal radiation is applied to the energy equation. Viscous dissipation will be neglected, leading to the following steady-state set of equations for velocity \mathbf{u} , pressure p and temperature T [4]:

$$\nabla \cdot \mathbf{u} = 0 \quad (1.6)$$

$$\nabla \mathbf{u} \cdot \mathbf{u} = -\nabla p + \nabla \cdot (\eta(\nabla \mathbf{u} + \nabla \mathbf{u}^T)) - \beta(T - T_{ref}) \mathbf{g} \quad (1.7)$$

$$\rho c_p \mathbf{u} \cdot \nabla T = \nabla \cdot (\lambda \nabla T) + \frac{\sigma}{2} \|\nabla V + i2\pi f \mathbf{A}\|^2 \quad (1.8)$$

where T_{ref} is an arbitrary reference temperature and $\|\cdot\|$ denotes the canonical Hermitian norm. The source term in the equation for temperature is the time-averaged Joule power density. No-slip condition is prescribed for the fluid velocity on all boundaries except for the surface of the melt, submitted to Marangoni stress. Eventually, the temperature field must satisfy heat flux equilibrium with the exterior on every boundary:

$$-\lambda \frac{\partial T}{\partial n} = h(T - T_{ext}) + \sigma_{SB} \epsilon (T^4 - T_{ext}^4) \quad (1.9)$$

Tab. 1. Parameters used for the CCIM modelling

Symbol	Property	Typical value
σ	Electrical conductivity	$\sim 10 \text{ S/m}$
f	Induction frequency	286 kHz
A_θ	Applied potential vector	$\sim 0.8 \text{ mT} \cdot \text{m}$
η_0, B, T_v	VFT parameters	see below
β	Thermal expansion	$6 \times 10^{-5} \text{ K}^{-1}$
ρ	Glass density	$2.76 \times 10^3 \text{ kg/m}^3$
c_p	Heat capacity	$\sim 1.6 \times 10^3 \text{ J/kg/K}$
λ	Effective thermal conductivity	$\sim 4 \text{ W/m/K}$
h	Thermal contact conductance	$15 \text{ W/m}^2/\text{K}$ (surface) $\sim 150 \text{ W/m}^2/\text{K}$ (other)
T_{ext}	External temperature	550 K (surface) 340 K (other)
ϵ	Emissivity	~ 0.4

1.3. Temperature estimator design

A scaling law can be derived from thermo-hydraulic equations using a boundary layer analysis, assuming forced convection regime and a VFT-like temperature-dependent glass viscosity [5]. Because of decreasing viscosity with increasing temperature, heat convection is strongly enhanced when increasing prescribed hot temperature. This behavior leads to stronger variations of heat flux with respect to

temperature difference than simple proportionality given by Newton's law. Let $\phi(T_h, \omega)$ be the heat flux received by any cooled sensor immersed in the melt for a prescribed glass hot temperature T_h (around mean temperature $\langle T_h \rangle$) and stirring rotational speed ω . The boundary layer analysis, not shown in this paper, leads to:

$$\phi(T_h, \omega) = \left(\frac{T_h - T_v}{\alpha} \right)^{1+\gamma} \omega^{1/2} \quad (1.10)$$

where γ depends only on the glass VFT parameters and the mean prescribed temperature (R stands for the universal gas constant):

$$\gamma = \frac{B}{3R(\langle T_h \rangle - T_v)} \quad (1.11)$$

and α is some scaling constant depending on the sensor geometry and other glass properties. Hence, we define the temperature estimator by inverting the scaling law:

$$\overline{T_h} = T_v + \alpha \left(\phi \omega^{-1/2} \right)^{1/(1+\gamma)} \quad (1.12)$$

Equation (1.12) is only valid for steady-states. The next section is dedicated to evaluating the scaling constant α for a particular sensor design using 3D coupled numerical simulation of the CCIM.

2. Sensor design and numerical simulation

2.1. Heat flux sensor

In our design, the heat flux sensor is a part of a cylindrical water-cooled stick made of stainless steel and immersed into the melt. The heat flux received by the measurement stick is computed from the temperature difference between incoming and outgoing cooling water. A good heat flux measurement needs a sufficiently high water temperature difference but must prevent any vaporization inside the sensor. Results of 3D coupled numerical simulations of

the CCIM shown in the following enabled a precise estimation of the heat flux, thus ensuring a proper sizing of the sensor in terms of rate of cooling.

2.2. Simulation strategy and results

Equations (1.1), (1.2), (1.6), (1.7) and (1.8) are solved simultaneously with a finite volume scheme using ANSYS ® Fluent. Equations (1.1) and (1.2) – written here for complex amplitudes – have been split into 8 real scalar equations and added to the software workflow using User Defined Functions. Couplings are solved with a segregated method until global convergence is reached. We used the embedded Multiple Reference Frame model to solve the stirrer steady rotational motion [6]. For a given value of stirring intensity $\omega = 5.29 \text{ rad/s}$, tuning the value of applied vector potential A_θ enables us to reach different values of glass temperature inside the melt, ranging from $1200 \text{ }^\circ\text{C}$ to $1300 \text{ }^\circ\text{C}$. For each temperature, one computes the total heat flux across the measuring stick boundary.

The glass used in the experiment is a French borosilicate simulant glass for the vitrification of fission products. Precise rheological measurements with varying temperature have been carried out on a small sample of glass. The later was found to follow very accurately the Vogel-Fulcher-Tamman law in the considered temperature range (see Fig. 1) with parameters:

$$\eta_0 = 1.16 \times 10^{-2} \text{ Pa} \cdot \text{s}, B = 3.32 \times 10^4 \text{ J/mol}, T_v = 586 \text{ }^\circ\text{C} \quad (2.1)$$

leading to the scaling law exponent $\gamma = 2.00$. Numerical simulations show very clearly that the behavior of heat flux with respect to prescribed hot temperature is in good agreement with the analytical scaling law, setting the scaling constant $\alpha \approx 55.9 \text{ SI}$ and $\langle T_h \rangle = 1250 \text{ }^\circ\text{C}$ (see Fig. 1 and 2).

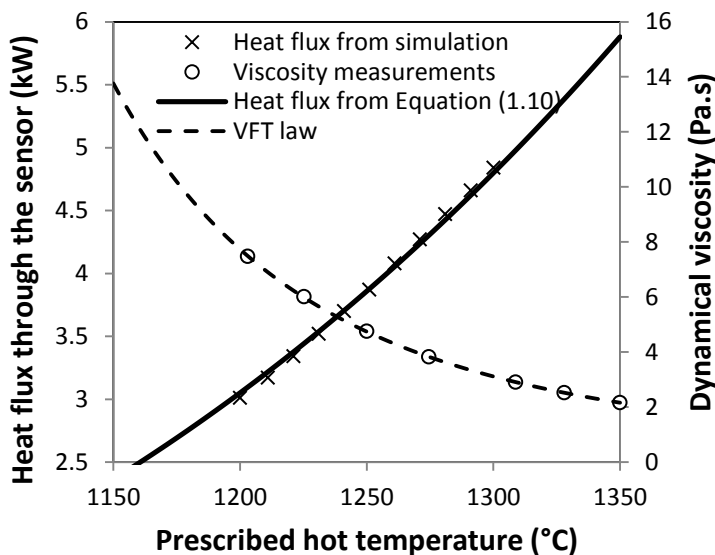


Fig. 1: Heat flux comparison between numerical results and analytical scaling law - viscosity change on the considered temperature range (measured values and VFT law)

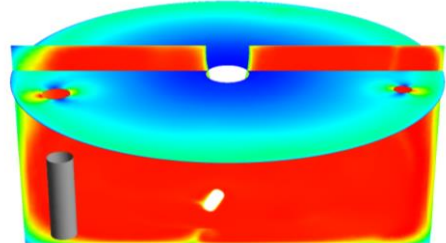


Fig. 2: Numerical simulation of the CCIM – horizontal cross section colored by Joule power density, vertical plane colored by temperature and envelop of heat flux sensor in gray color

3. Experimental validation

3.1. Experimental setup

The experiment consisted in the melting of around 300 kg of glass simulant. The CCIM was instrumented with both the heat flux sensor and a thermocouple sensor. The experiment lasted 24 hours and automatic measurements of temperature and heat flux were performed every 5 minutes. Temperature control was achieved with a PID controller governing the Joule power injected in the melt by the surrounding inductor. We prescribed different hot temperatures of the melt, starting with temperature 1290 °C down to 1200 °C with constant stirring rotational speed = 5.24 rad/s. Each 10°C decrease in the command was followed by a stabilization period of at least one hour. The glass melt was then heated up to 1300 °C. After stabilization, stirring intensity was decreased step by step down to 2.09 rad/s with stabilization plateaus.

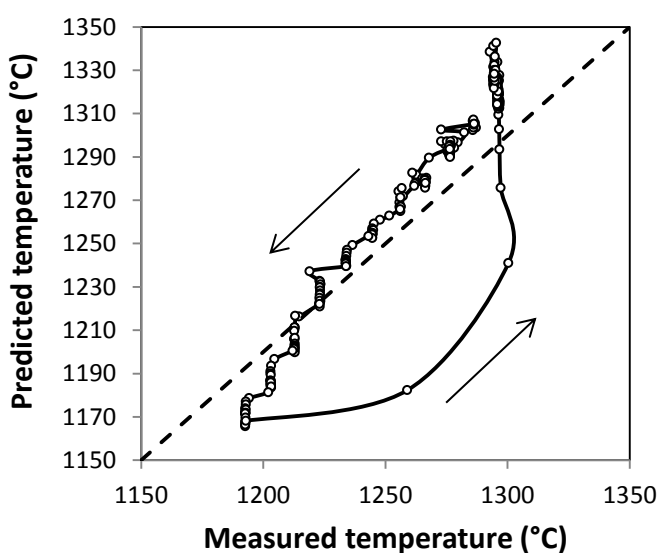


Fig. 3: Comparison between measured glass temperature and the estimator

satisfactory but shows a larger deviation, up to 40°C for the lowest stirring intensity. This overestimation is allegedly due to the fact that natural convection is no more negligible for low rotational speed. The contribution of free convection to the heat flux received by the sensor has indeed not been accounted for in the boundary layer analysis because of the assumption of forced convection regime. This assumption is however valid for high rotational speed, for which the Richardson number in the melt $Ri \propto \omega^{-2}$ is low enough (about 2×10^{-2}).

Conclusions

In this study, we used a Model and Simulation-based Systems Engineering approach to design a new indirect method of measuring glass temperature in a Cold Crucible Induction Melter used for High-Level-Waste vitrification purpose. The temperature is computed from real-time measurements of the heat flux received by a cooled sensor immersed in the melt, able to withstand strongly corrosive conditions. The temperature estimator has been derived from an analytical and numerical study of the magneto-thermo-hydraulic problem and shows a good agreement with the experimental data collected on a melting experiment where glass was strongly stirred using a mechanical cooled agitator. Contrary to classical thermocouple

3.2. Results

Fig. 3 shows the comparison between glass temperature given by the thermocouple sensor and predicted temperature \bar{T}_h obtained from heat flux measurements. A good agreement is observed with less than 20°C deviation during the first sequence, even during transient regimes following the change in prescribed temperature between plateaus. Strong deviation is observed when heating the melt back to higher temperatures, due to a strong misbalance between injected Joule power and heat fluxes from the melt to the cold crucible. For the second sequence, the behavior of the temperature estimator is

sensors, that need specific costly finger gloves to withstand hot glass flow, the sensor is reduced to a simple water-cooled tube made of steel. The observed deviation for low stirring rotational speeds observed in the experiments could be suppressed by using a boundary layer analysis in the mixed heat convection regime, thus accounting for free convection effects.

References

- [1] Badics, Z.: *Transient eddy current field of current forced three-dimensional conductors*. IEEE Transactions on magnetics, Vol. 28, 1992, pp. 1232–1234.
- [2] Biro, O., Preis, K.: *On the use of the magnetic vector potential in the finite element analysis of three-dimensional eddy currents*. IEEE Transactions on magnetics, Vol. 25, 1989, pp. 3145–3159.
- [3] Beckstein, P., Galindo, V., Gerbeth, G.: *Free-surface dynamics in the ribbon growth on substrate (rgs) process*. Proceedings of the International Conference on Heating by Electromagnetic Sources, Padua, 2016, pp. 127-134.
- [4] Bird, R. B., Stewart, W. E., Lightfoot, E. N.: *Transport Phenomena*. John Wiley & Sons, 2007, 905 pp.
- [5] Barba Rossa, G., Sauvage, E.: *Transfert thermique d'un fluide à viscosité thermo-dépendante vers une paroi refroidie*. Congrès Français de Thermique, Toulouse, 2016, 36.
- [6] ANSYS ® Fluent, Release 15.0, Help System, Theory Guide, ANSYS, Inc.

Authors

Barba Rossa, Guillaume
CEA, DEN, DE2D, SEVT, LDPV
Centre de Marcoule
F-30207 Bagnols-sur-Cèze
E-mail: guillaume.barbarossa@cea.fr

Sauvage, Emilien
CEA, DEN, DE2D, SEVT, LDPV
Centre de Marcoule
F-30207 Bagnols-sur-Cèze
E-mail: emilien.sauvage@cea.fr

Brun, Patrice
CEA, DEN, DE2D, SEVT, LDPV
Centre de Marcoule
F-30207 Bagnols-sur-Cèze
E-mail: patrice.brun@cea.fr